

1021 (1962).

¹⁵J. F. Koch, R. A. Stradling, and A. F. Kip, Phys. Rev. **133**, A240 (1954).¹⁶P. L. Taylor, Proc. Roy. Soc. (London), Ser. A **275**,

209 (1963).

¹⁷H. M. Rosenberg, Low Temperature Solid State Physics (Oxford University Press, London, England, 1963), Chap. 4, p. 93.

ULTRAVIOLET MAGNETO-OPTICAL PROPERTIES OF RARE-EARTH ORTHOFERRITES*

Frederic J. Kahn and P. S. Pershan†

Division of Engineering and Applied Physics, Harvard University, Cambridge, Massachusetts

and

J. P. Remeika

Bell Telephone Laboratories, Murray Hill, New Jersey

(Received 14 August 1968)

The first ultraviolet measurements of the complex polar Kerr effect (rotation and ellipticity) are reported between 1.8 and 5.5 eV for the rare-earth orthoferrites. The resonances observed are identified as charge transfer or charge-transfer-enhanced crystal-field transitions associated with octahedrally coordinated Fe³⁺ ions.

Since Dillon first observed large Faraday rotations associated with the visible absorption edge in rare-earth iron garnets,¹ there has been considerable interest in the optical properties of ferric oxide compounds.²⁻¹¹ Clogston discussed these phenomena in terms of electrical dipole allowed transitions, i.e., charge transfer and orbital promotion.² However, the strength of these transitions and the resulting opaqueness of these materials has prevented confirmation or elaboration of his theories.

Through the use of optical and magneto-optical (complex polar Kerr effect) reflection techniques, we have made the first observations of the ultraviolet spectra of bulk, single-crystal ferric oxide compounds.¹² We report here our results between 1.8 and 5.5 eV for europium orthoferrite, EuFeO₃. Measurements have also been made on rare-earth iron garnets, spinel ferrites, magnetoplumbite, nine additional rare-earth orthoferrites (RFeO₃, where R = Sm, Gd, Tb, Dy, Ho, Er, Tm, Yb, Lu), and YFeO₃. By application of these same techniques to the garnet system Eu₃Fe_{5-x}Ga_xO₁₂ (0 ≤ x ≤ 1.9), we have distinguished between the contributions of octahedrally and tetrahedrally coordinated Fe³⁺ ions. Furthermore, applying the results presented in this paper, we have shown that charge-transfer transitions occurring at about 4 and 5 eV, associated with octahedral and tetrahedral Fe³⁺ sites, respectively, are responsible for the principal features of the uv magneto-optical spectra of all the materials investigated.¹³ To our knowledge there have been no previous measurements of the com-

plex polar Kerr effect in the ultraviolet.¹⁴

Measurements were made near normal incidence and at room temperature on growth faces of crystals magnetized to saturation. Detailed investigations show that the properties measured are characteristic of the bulk rather than just the surface.¹³ While the spectrometer will be described elsewhere,¹⁵ typical signal-to-noise ratios are indicated by the error bars of Fig. 1(a). Our data are in good agreement with the results of Jung who measured the polar Kerr rotation, φ , and the diagonal element of the complex dielectric tensor, ϵ_0 , for ErFeO₃ in the visible range.⁸

The rare-earth orthoferrites, space group D_{2h}^{16} -Pbmm, have a distorted perovskite structure with only one type of Fe³⁺ ion site, Fe³⁺ octahedrally coordinated with O²⁻ ions.¹⁶ Nearest-neighbor Fe³⁺ ions are antiferromagnetically aligned, but a slight canting of the Fe³⁺ spins by an angle α on the order of 8 mrad creates a weak ferromagnetic moment.¹⁷ This net ordering of the spin system gives rise through spin-orbit coupling to the observed magneto-optical effects. The rare earths are only weakly coupled to the Fe³⁺ ions and at room temperature their magnetization can be neglected.¹⁷

Considering only effects linear in the magnetization \vec{M} , the complex dielectric tensor is of the form

$$\begin{aligned}\epsilon_{xx} &= \epsilon_{yy} = \epsilon_0' + i\epsilon_0'', \\ \epsilon_{xy} &= -\epsilon_{yx} = i(\epsilon_1' + i\epsilon_1''),\end{aligned}$$

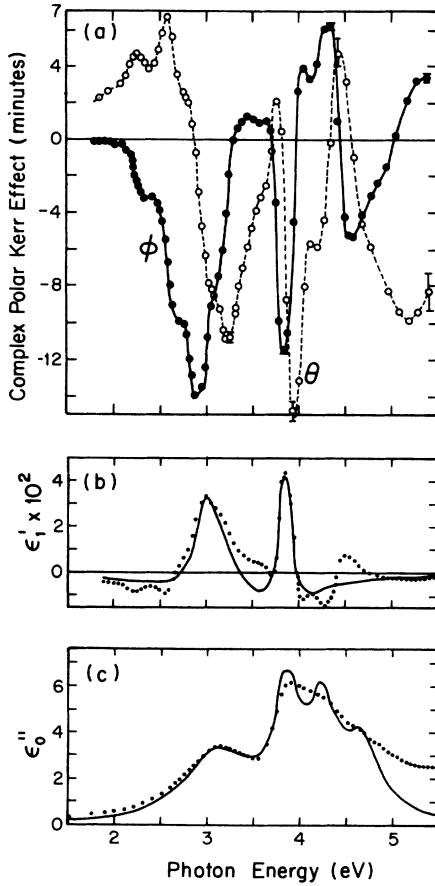


FIG. 1. Optical and magneto-optical results versus photon energy for a (001) face of EuFeO_3 . (a) Complex polar Kerr effect: rotation (ϕ) and ellipticity (θ). Values given are double rotations, and ellipticities, e.g., $\phi = \phi(\vec{M}) - \phi(-\vec{M})$. (b) Experimental (points) off-diagonal element ϵ_1' compared with theoretical (solid line) contribution from charge transfer transitions A-C. (c) Experimental (points) diagonal element ϵ_0'' compared with theoretical (solid line) contribution from charge transfer transitions A-E.

where \vec{M} and the wave vector \vec{k} are along z , ϵ_1 is linear in \vec{M} , ϵ_0 can be taken to be independent of \vec{M} , and $|\epsilon_1| \ll |\epsilon_0|$. The complex polar Kerr rotation Φ is defined by $\Phi = \phi + i\theta$, where ϕ is the rotation and θ the ellipticity. In terms of ϵ_1 and ϵ_0 ,¹⁸

$$\Phi = \phi + i\theta = -i\epsilon_1 [(\epsilon_0 - 1)\epsilon_0^{1/2}]^{-1}.$$

The diagonal elements $\epsilon_0'(\omega)$ and $\epsilon_0''(\omega)$ were obtained from a Kramers-Kronig analysis of reflectivity data taken up to 11 eV. Direct measurement of the rotation ϕ and the ellipticity θ determined the complex function $\Phi(\omega)$ from which the complex off-diagonal term $\epsilon_1(\omega)$ was calculated.¹⁸ Typical results for a (001) face of EuFeO_3

are shown in Fig. 1. The spectra for orthoferites vary only slightly with different rare earths and for our purposes can be regarded as independent of the rare earth. All of the observed transitions are therefore associated with the Fe^{+3} - O^{-2} sublattices.

The model proposed to explain the data follows Clogston's original treatment, except that it includes phenomenological damping constants that enable us to describe effects at, or close to, resonance. This is just the region where the most important spectral features are observed. Assuming a saturated spin system with an orbital singlet ground state (${}^6A_{1g}$) and N atoms per unit volume, the contribution of electric dipole transitions to the off-diagonal tensor elements will be given by^{18,19}

$$\epsilon_1 = \frac{2\pi N e^2}{\hbar} \sum_e \frac{(|r_{-ge}|^2 - |r_{+ge}|^2)(\omega - i\Gamma_{ge})}{\omega^2 - \omega_{eg}^2 - \Gamma_{ge}^2 - 2i\omega\Gamma_{ge}}, \quad (1)$$

where $r_{\pm ge} = \langle g | x \pm iy | e \rangle$, Γ_{ge} is the half-width at half-maximum for the contribution of the transition $|g\rangle - |e\rangle$ to $\epsilon_0''(\omega)$, and the sum is taken over all excited states $|e\rangle$.

The effect of spin-orbit coupling on allowed electric dipole transitions (${}^6A_{1g} - {}^6T_{1u}$) will be to lift the degeneracy of the transitions for left and right circularly polarized light, that is, for transitions to excited states with $m_L = \pm 1$. Application of Eq. (1) shows that this pair of transitions at energies $\hbar\omega_1$ and $\hbar\omega_2$ will provide a contribution to $\epsilon_1'(\omega)$ which is even about $\omega_0 = \frac{1}{2}(\omega_1 + \omega_2)$ and a contribution to $\epsilon_1''(\omega)$ which is odd about ω_0 . For $\Delta\omega < \Gamma$, where $\Delta\omega = \frac{1}{2}(\omega_1 - \omega_2)$ is the spin-orbit splitting, $\epsilon_1'(\omega)$ will be dissipative in shape and $\epsilon_1''(\omega)$ dispersive. Considering the two Fe^{3+} sublattices, we obtain $\epsilon_1 \max' = (\Delta\omega \sin\alpha) \times \Gamma^{-1} \epsilon_0 \max''$, where α is the canting angle of the Fe^{3+} spins. These results apply to the allowed electric dipole charge transfer and orbital promotion transitions discussed by Clogston.

The contribution to $\epsilon_1(\omega)$ from the spin- and parity-forbidden crystal-field transitions can similarly be calculated. Spin-orbit interaction, Fe^{3+} - Fe^{3+} interactions, lattice distortions, and other effects combine to make these transitions partially allowed. Their strength will be particularly enhanced if allowed electric dipole excitations, which can be admixed to relieve the parity constraint, lie close by in energy. For the ${}^6A_{1g} - {}^4T_{1g}$ crystal-field transition, the net result will be left and right circularly polarized transitions degenerate in energy but differing in

intensity. Application of Eq. (1) shows that the contributions to $\epsilon_1'(\omega)$ and $\epsilon_1''(\omega)$ will be, respectively, dispersive and dissipative in shape, just the opposite of our result for the allowed electric dipole transitions. Further details of the energy levels for this system will be discussed elsewhere.¹³

Assuming Lorentzian line shapes, the observed $\epsilon_1'(\omega)$ and $\epsilon_0''(\omega)$ can be explained by the transition assignments and associated parameters listed in Table I. The good agreement between the assignments and experiment is indicated by the theoretical curves of Figs. 1(b) and 1(c), where the contributions of charge-transfer transitions A-C to $\epsilon_1'(\omega)$ and A-E to $\epsilon_0''(\omega)$ are compared with the experimental spectra. The fit could undoubtedly be improved by further computation but the present agreement is most satisfactory. The line shapes of the resolved crystal-field transitions, dispersive in ϵ_1' and dissipative in ϵ_1'' , are consistent with our analysis.

One of the most important results of this study

is the observation, through the magneto-optical effects, of unresolved structure in the straight reflectivity spectra. Note, for example, transitions A, C, and f. Our identification of the absorption edge in the orthoferrites with charge transfer is in agreement with Grant's photoconductivity data on Gd iron garnet which shows *p*-type photoconductivity to be associated with this edge.²⁰

The experimental values in Table I for $2\Delta\omega \times \sin\alpha$, the spin-orbit splittings reduced to account for the canted antiferromagnetic alignment, are much larger for the charge-transfer excited states of transitions A, B, and C than for those of D and E, a result which aided in making the transition assignments. However, reconciliation of the absolute values with Clogston's estimates would require $\sin\alpha \approx 0.5$, whereas according to the currently accepted model $\sin\alpha = 0.008$ for EuFeO_3 .¹⁷ For ferrimagnetic ferric oxide compounds such as yttrium iron garnet, experimental values for ϵ_1' are of the same order of mag-

Table I. Summary of transition assignments including energies (*E*), oscillator strengths (*f*), linewidths (2Γ), tensor elements (ϵ_0'' and ϵ_1'), spin-orbit splittings ($2\Delta\omega$), and comparisons with estimated or calculated values where available.

Charge Transfer Transitions	E_{exp} (eV)	$2\Gamma_{\text{exp}}$ (eV)	$\epsilon_0''_{\text{max exp}}$	$\epsilon_1'_{\text{max exp}}$	f_{exp}	$(2\Delta\omega \sin\alpha)_{\text{exp}}$ ^a (cm ⁻¹)	f_{est} ^b	$2\Delta\omega_{\text{est}}$ ^b (cm ⁻¹)
A) $t_{2u}^n(\pi) \rightarrow t_{2g}^*$	3.0	.5	0.85	.023	.05	109	.13	175
B) $t_{1u}(\pi) \rightarrow t_{2g}^*$	3.15	.9	2.24	.013	.27	42	.13	175
C) $t_{1u}(\sigma) \rightarrow t_{2g}^*$	3.85	.3	4.18	.044	.20	25	.13	175
D) $t_{2u}^n(\pi) \rightarrow e_g^*$	4.25	.6	4.46	<.004	.47	<4.5	.40	<15
E) $t_{1u}(\pi) \rightarrow e_g^*$	4.70	.4	2.35	<.001	.18	<1.5	.40	<15
F) $t_{1u}(\sigma) \rightarrow e_g^*$	~5.25						.40	<15
Charge-Transfer-Enhanced			E_{exp}	E_{calc} ^c				
Crystal Field Transitions			(eV)	(eV)				
a) ${}^6A_{1g}({}^6S) \rightarrow {}^4E({}^4G), {}^4A_{1g}({}^4G)$			2.35	2.43				
b) ${}^6A_{1g}({}^6S) \rightarrow {}^4T_{2g}({}^4D)$			2.68	2.75				
c) ${}^6A_{1g}({}^6S) \rightarrow {}^4E_g({}^4P)$				3.09				
d) ${}^6A_{1g}({}^6S) \rightarrow {}^4T_{1g}({}^4P)$			3.60	3.69				
e) ${}^6A_{1g}({}^6S) \rightarrow {}^4A_{2g}({}^4F)$			4.10	4.12				
f) ${}^6A_{1g}({}^6S) \rightarrow {}^4T_{1g}({}^4F)$			4.40	4.59				

^aCanted antiferromagnetic alignment is accounted for by $\sin\alpha$ (see text).

^bSee Ref. 2.

^cSee Ref. 9.

nitude as for the orthoferrites.¹³ Since for these ferrimagnetic materials $\sin\alpha = 1$, $\Delta\omega \sin\alpha$ for these systems agrees with Clogston's estimates. The difference between the experimental and estimated values for $2\Delta\omega \sin\alpha$ in the orthoferrites is not understood at this time. More detailed molecular orbital treatments for these systems are urgently required in order to explain this apparent anomaly.

We would like to thank Mr. E. M. Kelly for assistance in crystal growth, Mr. Larry Ladd and Professor William Paul for their assistance with the straight reflectivity measurements, and Dr. Paul Grant of IBM, San Jose, for his Kramers-Kronig program.

*Work supported in part by the Joint Services Electronics Program (U. S. Army, U. S. Navy, and U. S. Air Force) under Contract No. N00014-67-A-0298-0006, by the Advanced Research Projects Agency SD-88, and by the Division of Engineering and Applied Physics, Harvard University, Cambridge, Mass.

†Alfred P. Sloan Foundation Fellow.

¹J. F. Dillon, Jr., *J. Phys. Radium* **20**, 374 (1959) and references cited therein.

²A. M. Clogston, *J. Phys. Radium* **20**, 151 (1959), and *J. Appl. Phys.* **31**, 198S (1960).

³R. C. Sherwood, J. P. Remeika, and H. J. Williams, *J. Appl. Phys.* **30**, 217 (1959).

⁴P. C. Bailey, *J. Appl. Phys.* **31**, 39S (1960). P. C. Bailey and A. Goldman, Westinghouse Research Laboratories Contract No. AF19(609)-5529, AD No. 240236.

⁵K. A. Wickersheim and R. A. Lefever, *J. Chem. Phys.* **36**, 844 (1962).

⁶C. A. Fowler, Jr., E. M. Fryer, B. L. Brandt, and R. A. Isaacson, *J. Appl. Phys.* **34**, 2064 (1963).

⁷R. L. Coren and M. H. Francombe, *J. Phys. Radium* **25**, 233 (1964).

⁸W. Jung, *J. Appl. Phys.* **36**, 1249 (1965).

⁹D. L. Wood and J. P. Remeika, *J. Appl. Phys.* **38**, 1038 (1967).

¹⁰P. M. Grant, *Appl. Phys. Letters* **11**, 166 (1967).

¹¹R. E. MacDonald, O. Voegeli, and C. D. Mee, *J. Appl. Phys.* **38**, 4101 (1967).

¹²Grant, Ref. 10, has independently measured the straight reflectivity of Gd iron garnet. Magneto-optical measurements, however, carry considerably more information than the straight reflectivity. Previous magneto-optical studies on ferric-oxide compounds were limited either to the visible range (Refs. 3, 4, 6, and 8) or to Faraday rotation of polycrystalline films (Refs. 7 and 11). The dielectric tensor elements necessary for full material characterization were obtained only by Jung (Ref. 8) who used Kramers-Kronig relations that were only valid for the region of weak absorption (private communication).

¹³F. J. Kahn, P. S. Pershan, and J. P. Remeika, to be published.

¹⁴For use of the equatorial Kerr effect to study Fe, Co, and Ni to 5 eV, see G. S. Krinchik, *J. Appl. Phys.* **35**, 1089 (1964).

¹⁵F. J. Kahn, to be published.

¹⁶S. Geller and E. A. Wood, *Acta Cryst.* **9**, 563 (1956); S. Geller, *J. Chem. Phys.* **24**, 1236 (1956).

¹⁷D. Treves, *J. Appl. Phys.* **36**, 1033 (1965).

¹⁸H. S. Bennett and E. A. Stern, *Phys. Rev.* **137**, A448 (1965).

¹⁹Y. R. Shen, *Phys. Rev.* **133**, A511 (1964).

²⁰P. M. Grant and W. Ruppel, *Solid State Commun.* **5**, 543 (1967).

GRAVITY-INDUCED ENERGY LOSSES IN MAGNETIC SUSPENSIONS

Titus Pankey, Jr.

Parabola Bluff, Charlottesville, Virginia

(Received 5 August 1968)

A horizontal magnetically suspended simple pendulum undergoes anomalous viscous damping nearly two orders of magnitude larger than observed in an identical vertical pendulum in a comparable magnetic field. A mathematical analysis of the experimental results infers that the energy losses are induced by gravity.

I recently published some experimental results¹ suggesting that the magnetic viscosities of suspended ferromagnetic masses (SM) were influenced by gravity. Some of the behavior described as anomalous lessened with the avoidance of body contact with SM immediately before suspension. An unexplained increase in viscosity with loading was still observed, however, and moreover these studies created an awareness of the need for basic research on the low-frequency

energy losses in magnetic suspensions.²

The suspension balance¹ is a horizontal spherical pendulum. Only one normal mode (vertical oscillations) is usually excited in the axial field of magnetron magnets with large plane poles. Stimulation of this mode at periods $T \geq 0.6$ sec is accompanied by an abnormally large logarithmic decrement (Table I) nearly 10^2 times the viscous losses in the constraining wire of 0.13-mm tungsten and from the atmosphere, deter-